# SUPPORTING INFORMATION FOR:

# Line Focused Optical Excitation of Parallel Acoustic Focused Sample Streams for High Volumetric and Analytical Rate Flow Cytometry.

Daniel M. Kalb,[1†] Frank A. Fencl,[1] Travis A. Woods,[1,2] August Swanson,[3] Gian C. Maestas,[1†] Jaime J. Juárez,[1†] Bruce S. Edwards,[2] *Andrew P. Shreve,[1] and *Steven W. Graves[1]

[1]Center for Biomedical Engineering & Department of Chemical and Biological Engineering, University of New Mexico, Albuquerque, NM 87131

[2]Center for Molecular Discovery, Innovation Discovery and Training Center, Health Sciences Center, University of New Mexico, Albuquerque, New Mexico, 87131-0001 United States

[3]DarklingX, Los Alamos, NM 87544, USA

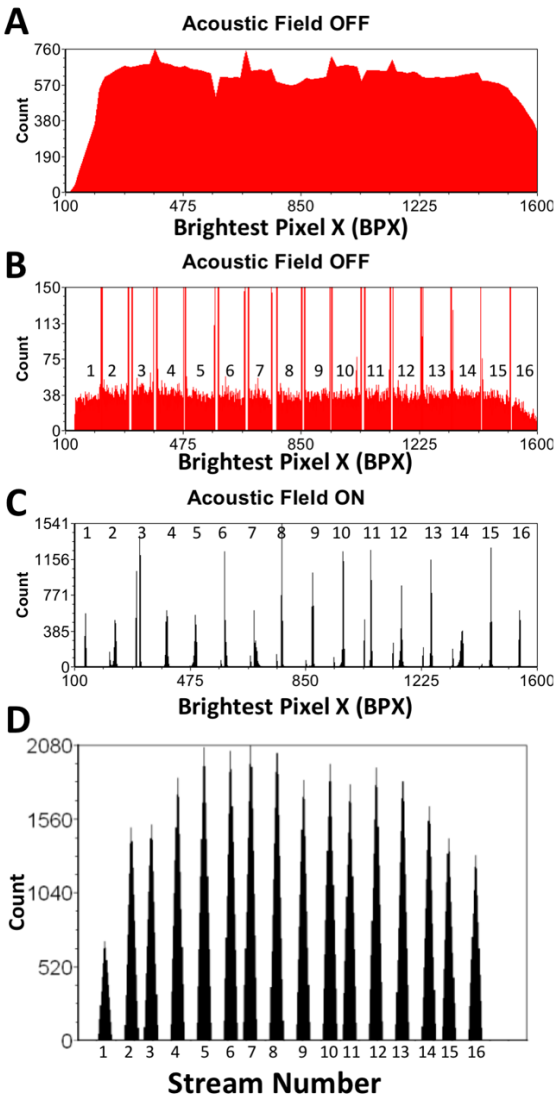


**Figure S-1. Acoustic focusing across the channel width of flowing 6 µm microspheres.** (A) The X location of brightest pixel of each event for unfocused fluorescent microspheres flowing through the system. In this data a single broad window that encompassed the entire channel was assigned. Therefore, when an event occurs its X location is recorded simply as the location of the brightest pixel. This even distribution of events shows that we have laminar flow within the channel. (B) Using estimates of positions as determined by visualization of the channel (Figure 1E), we assigned 16 windows for data collection. Each window began with a minimal pixel and a maximal pixel as described in Figure 3A. The window numbers are shown on the in black text, 1 – 16. This shows the collection of data for unfocused particles. As such, there are large numbers of particles across each X position of each window. The increase in number of particles at the edge of each window is due to particles being recorded in the edge pixel of each window as they pass by in areas of the sensor that were not directly addressed by the window. Such particles will have their brightest pixel recorded as the edge pixel, which increases the number of events in the edge pixels. (C) Focused particles flowing in the defined windows. The application of the acoustic focusing generated 16 nodes that position almost all of the particles in specific areas of the sensor as recorded by the BPX value. Though some streams (e.g. stream 3) show some variation of position resulting from small shifts of the particles as they flow, acoustic focusing clearly tightly positions particles into 16 streams across the flow cell. (D). Using focused particles, the 16 windows are used to assign corresponding stream numbers to microspheres as they flow through the analysis region. The stream number parameter is a simple method to select populations of particles based on which stream they occur within. The data also shows that similar numbers of particles occur within each stream. While we have not extensively characterized the flow pattern of our system, the number of events in each stream are suggestive of a parabolic flow pattern. However, such a pattern is not expected to form using the wide but shallow channel (2300 µm wide by 200 µm deep) used here.[1] Rather than a fluidic effect, we hypothesize that the fall off of number of events is likely due to reduced sensitivity on the edge channels caused by optical vignetting. Reduced sensitivity would result in any dimmer particles potentially falling below our trigger threshold, which would cause a correspondingly lower number of events to be detected.

(1) Stone, H. A. In CMOS Biotechnology; Springer, 2007, pp 5-30.

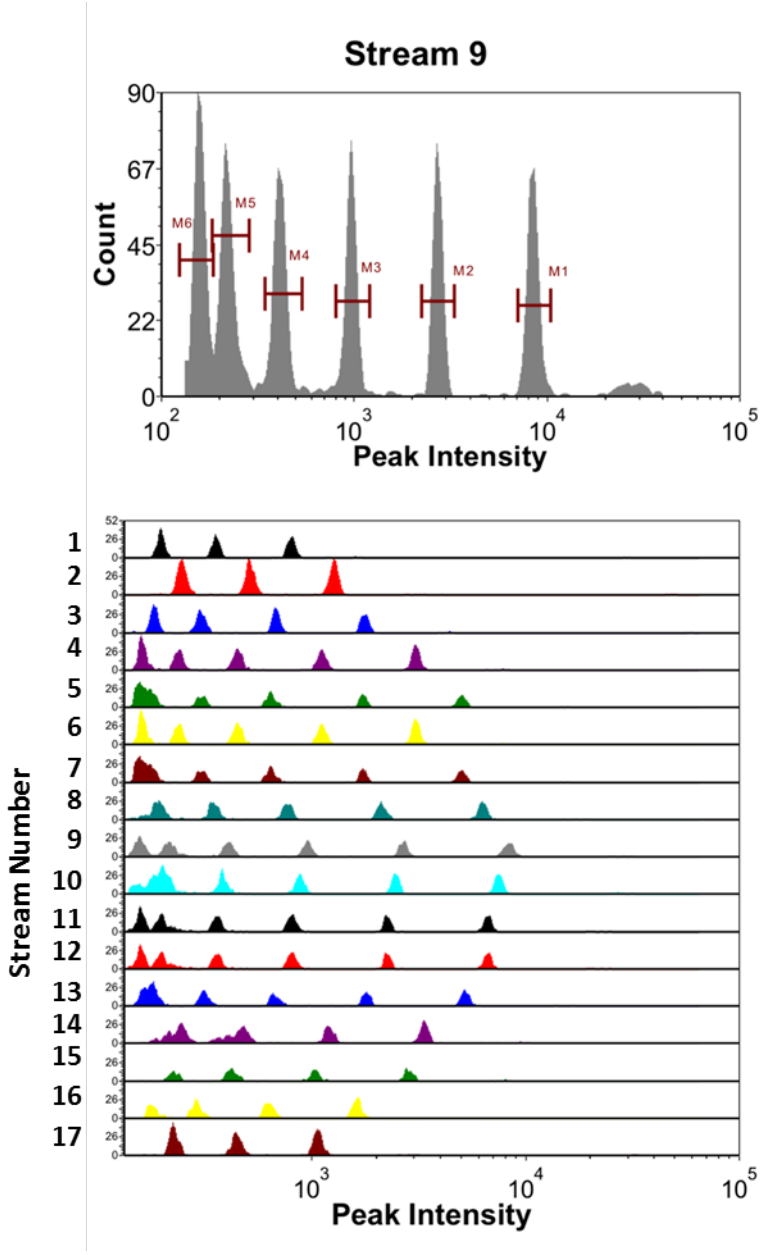


**Figure S-2. Histograms of six-peak rainbow beads**. The best performing stream (top) and all of the streams (bottom) with 6 μm calibration beads (RCP-60-5, Spherotech, Lake Forest, IL). Six peak rainbow calibration beads were used as a calibration standard to characterize the performance of our cytometer. The five fluorescent peaks are clearly visible in the center of the channel with CV's comparable to those acquired on a commercial flow cytometer (4-6%) and are clearly distinguishable from each other. It is also promising that we appear to see the population of blank beads, but further analysis is needed to confirm this. It should be noted that in this data set we operated the system at a PZT drive frequency of 5.32 MHz to create 17 streams, rather than the 16 streams used in the data presented in the main manuscript.

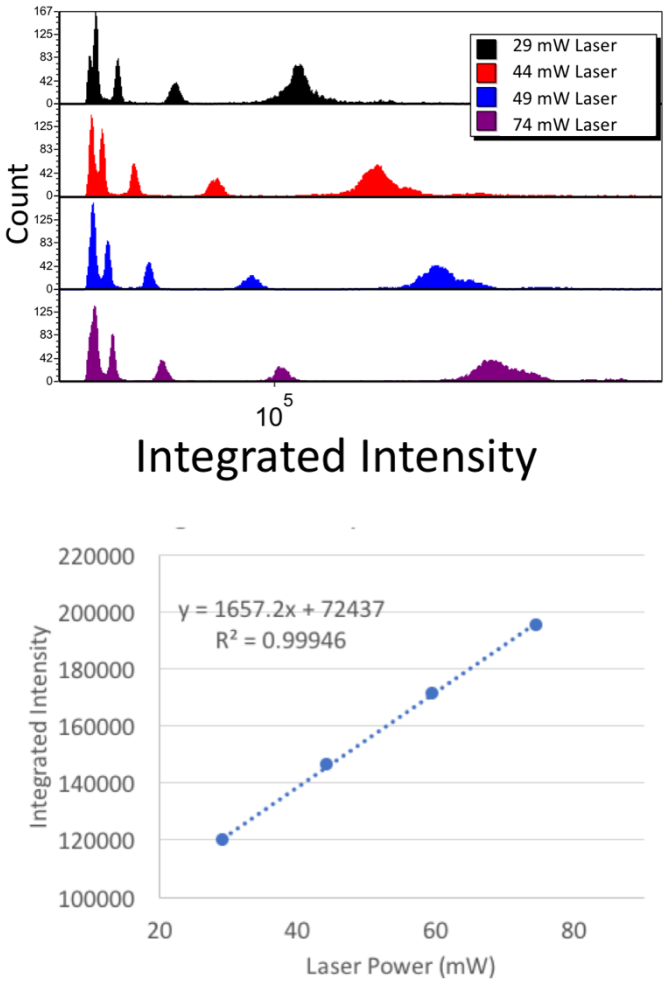


**Figure S-3. Linear relationship of laser power to the fluorescence intensity collected by the system. Top** For a 6-peak bead population, we see that all bead populations increase in fluorescent intensity with applied laser power. **Bottom:** The peak intensity of the brightest bead of the population increases with applied laser power. With a relatively constant background noise, this leads to increased sensitivity with applied laser power.

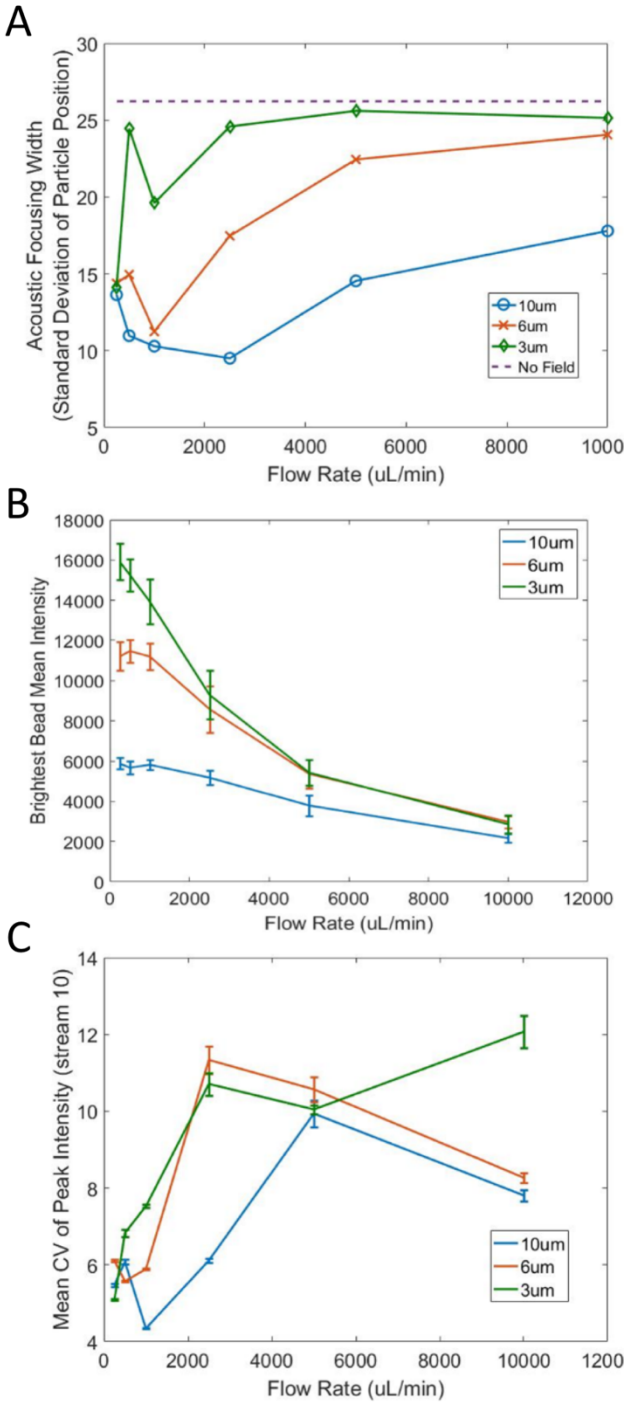


**Figure S-4. Performance of standard beads vs. flow rate.** (A) Focusing width (standard deviation of particle position relative to the mean particle position in each mode, averaged over all particle streams) vs. flow rate. (B) Mean intensity of the brightest bead population across flow rate. (C) Mean CV of all bead populations in stream 10 across flow rate.

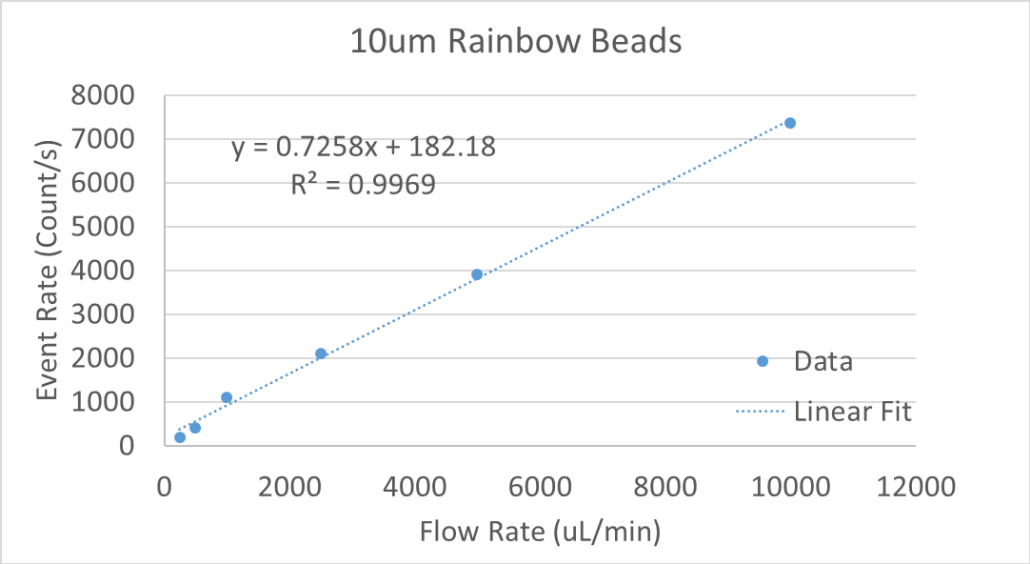


**Figure S-5.** For a constant bead input, we see a linear relationship between event rate and input flow rate. This suggests that we are seeing all beads across the range of flow rates. We are not missing the fastest flowing beads at the highest flow rates.

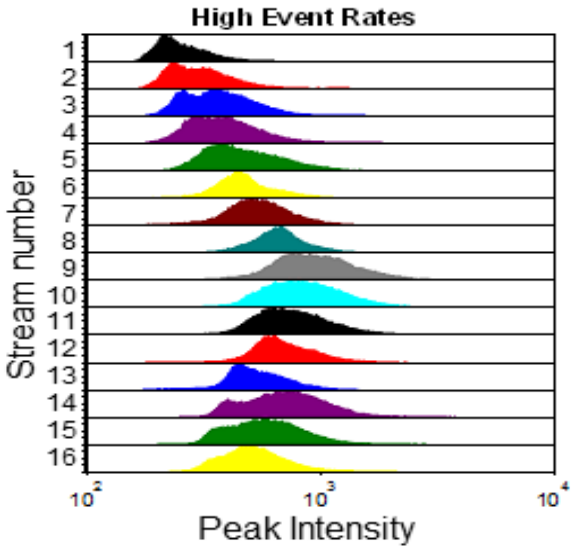


**Figure S-6. High event rate data for 6 µm Nile red beads.** At 10 mL/min there are 957,366 events within 9.4 seconds, yielding an analytical event rate of ~102k/s